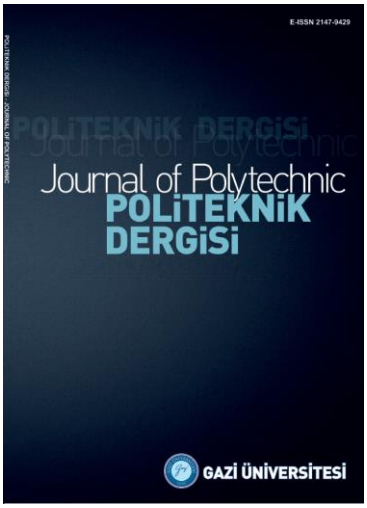

POLİTEKNİK DERGİSİ

JOURNAL of POLYTECHNIC

ISSN: 1302-0900 (PRINT), ISSN: 2147-9429 (ONLINE)
URL: http://dergipark.org.tr/politeknik

A comparison of circular duct and real hexagonal duct results using hydraulic diameter

Hidrolik çap kullanarak dairesel kanal ve gerçek altıgen kanal sonuçlarının karşılaştırılması

***Yazar(lar) (Author(s))**: Umut Barış YILMAZ[1], Oğuz TURGUT[2]*

ORCID[1]: 0000-0002-6103-7670

ORCID[2]: 0000-0001-5480-1039

Bu makaleye şu şekilde atıfta bulunabilirsiniz(To cite to this article): Yilmaz U. B. and Turgut O., "A comparison of circular duct and real hexagonal duct results using hydraulic diameter", ***Politeknik Dergisi***, 24(4): 1593-1604, (2021).

Erişim linki (To link to this article): http://dergipark.org.tr/politeknik/archive

DOI: **10.2339/politeknik.768211**

A Comparison Of Circular Duct And Real Hexagonal Duct Results Using Hydraulic Diameter

Hidrolik Çap Kullanarak Dairesel Kanal ve Gerçek Altıgen Kanal Sonuçlarının Karşılaştırılması

Highlights

- *A numerical study has been conducted whether the correlations derived for circular duct can be used for hexagonal ducts or not.*
- *The effects of Reynolds number and side angle of the duct on heat transfer and flow characteristics have been investigated.*
- *Minimum pressure loss and maximum heat transfer are obtained for regular hexagonal duct.*
- *General correlations are given for Nusselt number and friction factor.*

Graphical Abstract

Turbulent flow in a hexagonal duct has been investigated numerically in order to see whether the correlations given for circular ducts can be used for hexagonal ducts or not.

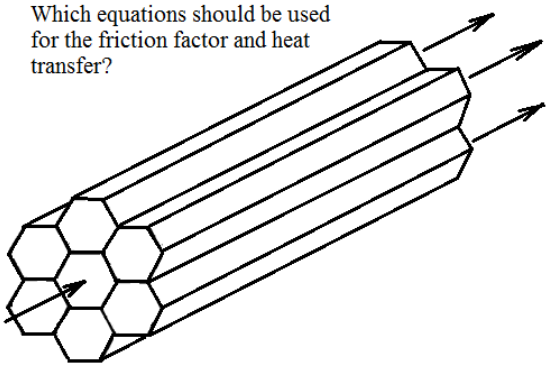

Figure. Hexagonal duct

Aim

The aim of this study is to see whether the correlations given for circular ducts can be used for hexagonal ducts or not.

Design & Methodology

A numerical study has been conducted using ANSYS Fluent 17.0 software. Study has been carried out for the Reynolds number between $10\times10^3 \leq Re \leq 50\times10^3$ and side angle of the duct varying between 30^o and 90^o.

Originality

Novelty of this study is the examination of hydrodynamically fully developed, thermally developing turbulent heat transfer and fluid flow in a hexagonal cross-sectional duct.

Findings

It is found that using correlations of circular ducts for hexagonal ducts employing hydraulic diameter may be 5% and 14% higher than that of actual hexagonal cross-sectional channels for Nusselt number and Darcy friction factor, respectively. Side angle of hexagonal duct affects the pressure drop along duct and heat transfer coefficient.

Conclusion

General correlations are given in terms of Reynolds number and side angle for Nusselt number within –10.8% and +4.5% and Darcy friction factor within –6.0% and +0.2%. Minimum pressure drop and maximum Nusselt number in hexagonal-shaped cross-sectional duct are obtained for regular hexagonal duct, $\theta=60^o$.

Declaration of Ethical Standards

The author(s) of this article declare that the materials and methods used in this study do not require ethical committee permission and/or legal-special permission.

A Comparison of Circular Duct and Real Hexagonal Duct Results Using Hydraulic Diameter

Araştırma Makalesi / Research Article

Umut Baris YILMAZ[1], Oguz TURGUT[2*]

[1]Yuksel Proje A.S., Birlik Mahallesi 450. Cadde No: 23, 06610 Cankaya, Ankara, Turkey
[2]Gazi University, Faculty of Engineering, Department of Mechanical Engineering & Clean Energy Research and Application Center (TEMENAR), Maltepe, Ankara, Turkey

(Geliş/Received : 11.07.2020 ; Kabul/Accepted : 07.10.2020 ; Erken Görünüm/Early View : 24.11.2020)

ABSTRACT

To see whether the turbulent flow correlations derived for circular ducts can be used for hexagonal cross-sectional ducts using hydraulic diameter, turbulent flow in hexagonal ducts is numerically investigated under constant wall temperature boundary condition using ANSYS Fluent 17.0 software. Investigated parameters are the Reynolds number between $10\times10^3\leq Re\leq50\times10^3$ and side angle of the duct varying between 30^o and 90^o. Standard k-ε model is used as turbulence model. General expressions are proposed for fully developed dimensionless heat transfer coefficient Nusselt number and fully developed Darcy friction factor in terms of Reynolds number and side angle for hexagonal-shaped cross-sectional duct. Results show that side angle of hexagonal duct affects the pressure drop along duct and heat transfer coefficient in duct. Results point out that regular hexagonal duct, $\theta=60^o$, gives minimum pressure drop and maximum Nusselt number. It is concluded that correlations given in the literature for circular ducts in turbulent flow can give 14% higher dimensionless heat transfer coefficient, Nusselt number, than that of actual hexagonal duct flow.

Keywords: Hexagonal duct, heat transfer, turbulent flow, numerical analysis.

Hidrolik Çap Kullanarak Dairesel Kanal ve Gerçek Altıgen Kanal Sonuçlarının Karşılaştırılması

ÖZ

Dairesel kanallar için türetilmiş türbülanslı akış korelasyonlarının hidrolik çap kullanılarak altıgen kesitli kanallar için kullanılıp kullanılamayacağını görmek için ANSYS Fluent 17.0 yazılımı kullanılarak altıgen kanallardaki türbülanslı akış sayısal olarak incelenmiştir. 30^o ile 90^o arasında kanal yanal açıları ve $10\times10^3\leq Re\leq50\times10^3$ arasındaki Reynolds sayısı parametreleri incelenmiştir. Türbülans modeli olarak standart k-ε modeli kullanılmıştır. Altıgen kesitli kanallar için Reynolds sayısına ve yanal açıya bağlı tam gelişmiş boyutsuz ısı transfer katsayısı olan Nusselt sayısı ve tam gelişmiş Darcy sürtünme faktörü için genel ifadeler önerilmiştir. Sonuçlar, altıgen kanal yanal açısının kanal boyunca basınç düşümünü ve kanaldaki ısı transfer katsayısını etkilediğini göstermiştir. Ayrıca sonuçlar $\theta=60^o$ olan eşkenar altıgen kanalın minimum basınç düşüşü ve maksimum Nusselt sayısı verdiğini göstermiştir. Literatürde türbülanslı akış koşullarında dairesel kanallar için verilen korelasyonların gerçek altıgen kanal akışına göre %14 daha yüksek boyutsuz ısı transfer katsayısı olan Nusselt sayısı sağlayabileceği sonucuna varılmıştır.

Anahtar Kelimeler: Altıgen kesitli kanal, ısı transferi, türbülanslı akış, sayısal analiz.

1. INTRODUCTION

Flow behavior in channels and the amount of heat transfer between duct walls and fluid are the significant topics of thermal engineering. Specifically, channel geometry plays an important role for applications. Non-circular ducts are preferred in compact heat exchangers as they increase forced convection and thus heat transfer coefficient. The turbulent flow correlations for circular ducts are commonly employed in noncircular ducts employing hydraulic diameter. However, the conclusions of both heat transfer coefficient and friction factor determined from circular duct expressions can be up to 35% higher than the results of real non-circular duct fluid flow [1-2].

*Sorumlu Yazar (Corresponding Author)
e-posta : oturgut2006@gmail.com

Hexagonal-shaped cross-sectional channels are generally encountered in nuclear engineering applications, waste heat recovery, cooling systems of electronic devices and lamella type compact heat exchangers used in many industries such as paper, alcohol, petrochemical and food [3].

Literature review shows that laminar [2-18] and turbulent [19-29] heat transfer and fluid flow in hexagonal channels are examined by some researchers. Rokni and Gatski [19] predicted turbulent heat transfer and turbulent fluid flow in non-circular channels including rectangular cross-sectional duct with aspect ratio 2. Sari [20] experimentally investigated steady-state both thermally and hydrodynamically developing turbulent fluid flow in a regular hexagonal-shaped cross-sectional duct for the constant wall temperature boundary condition at the Reynolds number range $2322\leq Re\leq8980$.

A numerical investigation was carried out by Can et al. [21] for turbulent flow in hexagonal channels for the Reynolds number of 20,000. Turgut and Sari [22] experimentally and numerically investigated the thermally and hydrodynamically developing turbulent air flow in a regular hexagonal-shaped cross-sectional channel for Reynolds number $2.3\times10^3\leq Re\leq53\times10^3$ for two different k-omega and three different k-ε turbulence models. Turbulent flow and heat transfer in non-circular ducts including equilateral triangle, square, regular hexagon, regular octagon, regular dodecanon were numerically investigated by Wang et al. [23] using air as the working fluid for the Reynolds number of 53,477. It was concluded that standard k-ε turbulence model gives good aggreement with the available experimental data. Opute [24] studied experimentally laminar and turbulent flow and heat transfer in hexagonal tubes for SiO_2-water nanofluid in the Reynolds number range of 4000<Re<8000. Falih [25] examined the turbulent heat transfer and turbulent fluid flow inside a horizontal hexagonal-shaped cross-sectional channel fitted with combined wire coil turbulators and a perforated twisted-tape swirl generator. Marin et al. [26] numerically investigated turbulent flow in hexagonal ducts using large-eddy simulation and direct numerical simulation models. Gunes et al. [27] performed a numerical study to examine the heat transfer and fluid flow in a tube with hexagonal cross-sectioned coiled wire for the Reynolds number range of 5000<Re<17,000. Mahato et al. [28] conducted a numerical study to investigate the turbulent flow and heat transfer in hexagonal twisted duct. Turbulent heat transfer and fluid flow in a hexagonal duct with twisted-tape inserts were examined experimentally by Yadav et al. [29].

Literature study indicates a lack of knowledge about the characteristics of turbulent heat transfer and turbulent fluid flow in hexagonal-shaped cross-sectional channels. Therefore, in this present study, hydrodynamically fully developed and thermally developing turbulent fluid flow and convective heat transfer in hexagonal-shaped cross-sectional duct are numerically studied at constant wall temperature boundary condition. Investigated parameters are the Reynolds number ranging between $10\times10^3\leq Re\leq50\times10^3$, and side angle varying from 30° to 90° with an incremental of 15°. ANSYS Fluent 17.0 software package is employed for the numerical studies. Novelty of this present numerical study is the examination of hydrodynamically fully developed, thermally developing turbulent heat transfer and fluid flow in a hexagonal cross-sectional channel for different side angles and Reynolds numbers.

2. NUMERICAL STUDY

2.1. Mathematical Model and Governing Equations

Hydrodynamically fully developed and thermally developing turbulent heat transfer and fluid flow inside a hexagonal-shaped cross-sectional channel are studied under constant temperature boundary condition. Flow geometry consists of an entrance section duct and a test section duct as seen in Fig. 1a. In order to obtain a hydrodynamically fully developed flow regime at the exit of the entrance section duct, entrance section length is selected as 2.65 m. That is, hydrodynamically fully developed fluid enters the inlet section of the test section channel. That is, entrance duct has enough length to obtain hydrodynamically fully developed condition at the exit section. One side length of hexagonal duct is selected as 0.030 m. In other words, heat transfer area is kept constant when side angle is changed. Test section length is taken as 2 m. Studies are performed for five different channels with different edge angles θ changing between 30° and 90° with an incremental of 15°. Channel with θ=90° corresponds to a rectangular-shaped cross-sectional duct with aspect ratio 2, and hexagonal duct with θ=60° is called regular duct. Air having a Prandtl number 0.7 is employed as working fluid. Fluid flows in the positive x-direction.

Since the model has a symmetry on x-y and x-z planes, only a quarter of hexagonal cross-sectional duct is used as computational domain as shown in Fig. 1b. The Navier–Stokes equations have been employed in order to model the heat transfer and fluid flow in the computational region. Energy, momentum and continuity equations are the governing equations in numerical study. Fluid is modeled as incompressible, constant property, steady state, and Newtonian. Buoyancy effects and viscous dissipation are neglected. Using assumptions stated above the governing equations are expressed as:

$$\text{Continuity: } \frac{\partial}{\partial x_i}\left(\rho\overline{u_i}\right)=0 \tag{1}$$

Momentum:

$$\frac{\partial}{\partial x_j}\left(\rho\overline{u_j u_i}\right)=-\frac{\partial\overline{P}}{\partial x_i}+\frac{\partial}{\partial x_j}\left[\mu\left(\frac{\partial\overline{u_i}}{\partial x_j}+\frac{\partial\overline{u_j}}{\partial x_i}\right)\right]+\frac{\partial}{\partial x_j}\left(-\rho\overline{u_i' u_j'}\right) \tag{2}$$

$$\text{Energy: } \frac{\partial}{\partial x_j}\left(\rho\overline{u_j T}\right)=\frac{\partial}{\partial x_j}\left(\frac{\mu}{Pr}\frac{\partial\overline{T}}{\partial x_j}\right)-\rho\overline{u_j' T'} \tag{3}$$

Average Reynolds stress $\left(-\rho\overline{u_i' u_j'}\right)$ in momentum equation and turbulent heat flux $\rho\overline{u_j' T'}$ in energy equation are expressed by a suitable turbulence model. The Reynolds stress is expressed as follows:

$$R_{ij}=-\rho\overline{u_i u_j}=-\rho\frac{2}{3}k\delta_{ij}+\mu_t\left(\frac{\partial\overline{u_i}}{\partial x_j}+\frac{\partial\overline{u_j}}{\partial x_i}\right) \tag{4}$$

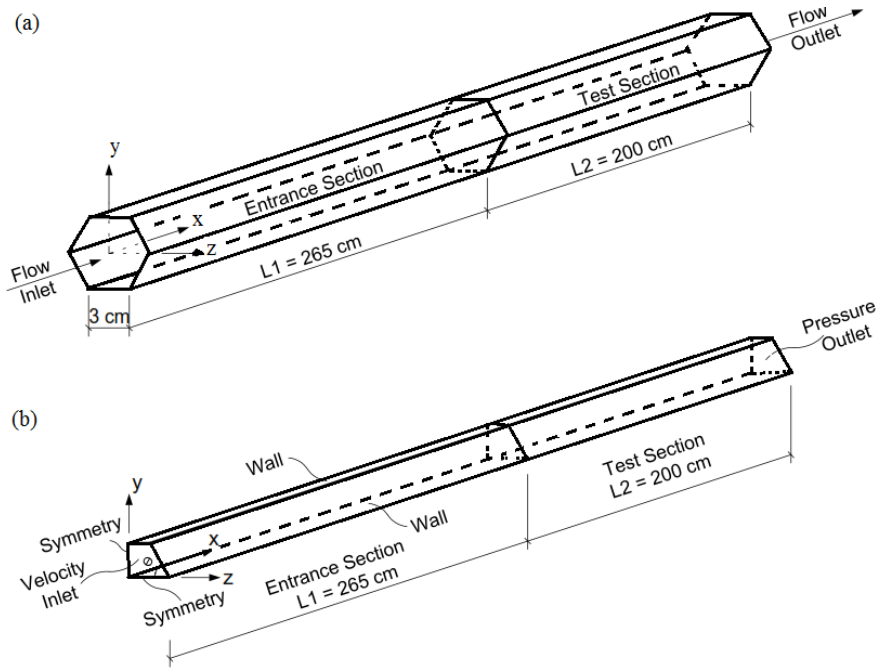

Figure 1. (a) Hexagonal duct used; (b) Computational domain and boundary conditions

Choosing of appropriate turbulence model is significant in order to study the turbulent flow and heat transfer in duct. Literature review showed that standard k-ε turbulence model was proven to be the appropriate turbulence model for the flow in non-circular ducts [23, 30-35]. Therefore, in this study, standard k-ε turbulence model was used due to its economy, robustness, and reasonable accuracy [36].

Equations given above are solved together with the standard k-ε turbulence model equations:

$$\frac{\partial}{\partial x_i}\left(\rho k\overline{u_i}\right)=\frac{\partial}{\partial x_j}\left[\left(\mu+\frac{\mu_t}{\sigma_k}\right)\frac{\partial \varepsilon}{\partial x_j}\right]+G_k-\rho\varepsilon \tag{5}$$

$$\frac{\partial}{\partial x_i}\left(\rho\varepsilon\overline{u_i}\right)=\frac{\partial}{\partial x_j}\left[\left(\mu+\frac{\mu_t}{\sigma_\varepsilon}\right)\frac{\partial \varepsilon}{\partial x_j}\right]+c_{1\varepsilon}\frac{\varepsilon}{k}G_k - c_{2\varepsilon}\rho\,\varepsilon^2/k \tag{6}$$

where G_k is the turbulence kinetic energy generation and given as:

$$G_k=\left(-\rho\overline{u_i'u_j'}\right)\frac{\partial\overline{u_j}}{\partial x_i} \tag{7}$$

In Eq. (6), $C_{\varepsilon 1}$ and $C_{\varepsilon 2}$ are the turbulence model constants, and their values are 1.44 and 1.92, respectively. These equations are solved together with appropriate boundary conditions. Boundary conditions employed in the numerical studies are depicted in Fig. 1b. At x=0, air as fluid goes into the entrance section channel at a uniform velocity. Pressure outlet boundary condition is employed at the exit of the entrance section channel, that is, at x=L1 [36]. No-slip velocity boundary condition is employed at the entrance section channel walls. Symmetry boundary condition is employed to y=0 and z=0 planes. The turbulence kinetic energy k and the turbulence dissipation rate ε at x=0 are calculated from the following equations:

$$k=0.005U_i^{\,2} \text{ and } \varepsilon=0.1643k^2/(0.07D_h) \tag{8}$$

At the exit of the entrance section channel, the values of necessary parameters attained from numerical study are written in a file. Then, the knowledge in this file is read at the inlet of the test section channel as input to reduce the mesh number and save computational time. Air goes into the hexagonal-shaped cross-sectional test section channel at a uniform temperature 300K. To the walls of the test section channel, constant temperature boundary condition, T_w=325K, is given. At the exit of test section channel, pressure outlet boundary condition is employed [36]. Fluid properties are taken at 300K and assumed as constant in computational domain [37]. Turbulence viscosity is indirectly solved by the transport equation of the modified viscosity in single-equation models. In two-equation models, the turbulence viscosity is associated with the turbulence kinetic energy (k) and the turbulence dissipation rate (ε) and is expressed as follows:

$$\mu_t=\rho C_\mu k^2/\varepsilon \tag{9}$$

Reynolds number based on inlet velocity and hydraulic diameter is given as:

$$\mathrm{Re}=\rho U_i D_h/\mu \tag{10}$$

where D_h is the hydraulic diameter, and it is the ratio of four times cross-sectional area to the wetted perimeter. Local dimensionless heat transfer coefficient Nusselt number is determined from:

$$Nu_x = h_x D_h / k \quad (11)$$

Here h_x is the local heat transfer coefficient and determined as:

$$h_x = \dot{q}''_x / (T_w - T_b)_x \quad (12)$$

Mean Nusselt number is calculated as:

$$Nu = hD_h / k \quad (13)$$

Here, h ($W \cdot m^{-2} \cdot K^{-1}$) is the mean convection heat transfer coefficient in the hexagonal-shaped cross-sectional channel, and it is obtained as:

$$h = \dot{m} c_p (T_o - T_i) / A_s \Delta T_{ln} \quad (14)$$

where:

$$\Delta T_{ln} = \frac{(T_w - T_i) - (T_w - T_o)}{\ln[(T_w - T_i)/(T_w - T_o)]} \quad (15)$$

Here ΔT_{ln} is the logarithmic average temperature difference. T_i, T_w, and T_o (K) are the inlet, the wall, and the outlet temperatures, respectively. The peripherally mean local Darcy friction factor f_x is expressed as:

$$f_x = 8\tau_{w,x} / \rho U_i^2 \quad (16)$$

where $\tau_{w,x}$ is the peripherally averaged shear stress on the wall at any axial location x. Mean Darcy friction factor is calculated as:

$$f = \frac{D_h}{L} \frac{\Delta P}{\rho U_i^2 / 2} \quad (17)$$

2.2. Numerical Procedure

Numerical study is implemented employing ANSYS Fluent 17.0 software program which uses finite volume approach to calculate the flow parameters. Standard k-ε turbulence model, proposed by Launder and Spalding [36], with enhanced wall treatment was used in the numerical study. SIMPLE algorithm is employed to resolve pressure–velocity coupling. Convective terms have been discretized employing second-order upwind scheme. Momentum, mass, energy, and turbulence equations have been iterated until the residual drops below 10^{-6} in order to obtain convergence. To obtain mesh independency, mesh optimization is conducted. The y+ value is taken about unity near the wall. For all numerical solutions, non-uniform hexagonal meshes are selected. A typical view of mesh distribution is given in Fig. 2. As can be seen in Fig. 2, smaller meshes are used towards the two edges (upper and right side walls) and two symmetry planes (left and bottom planes) of hexagon. That is, fine grids are employed on the two walls of the computational domain as seen in Fig. 2a and 2b.

A grid independence study is conducted by varying mesh (cell) size within the numerical computational region for Reynolds number 50×10^3 until the variation in mean Darcy friction factor and mean Nusselt number are less than 1%. Typical variation of mean Nusselt number and mean Darcy friction factor with different mesh numbers at Re=50×10^3 are given in Table 1 for hexagonal duct with side angle 60°, regular hexagonal duct.

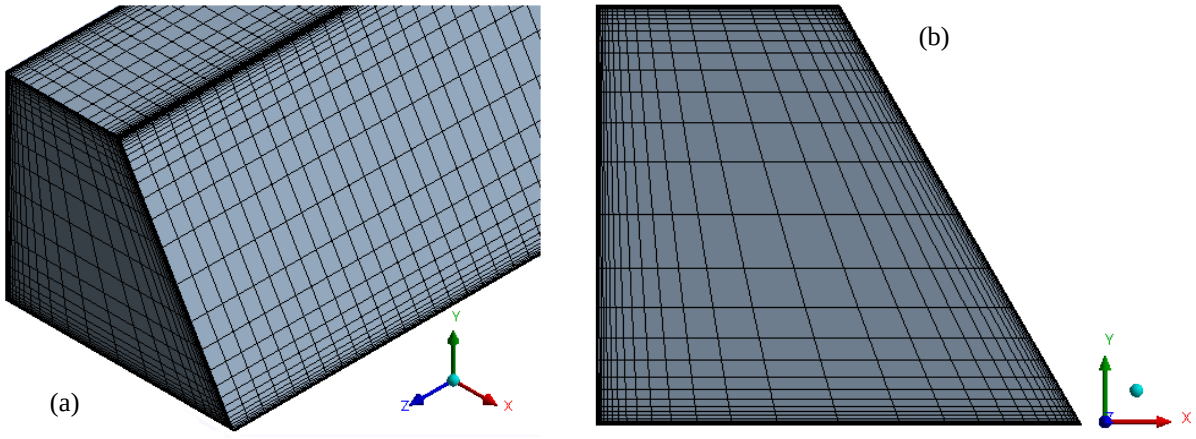

Figure 2. (a) Isometric and (b) side view of grid structure of hexagonal duct

Table 1. Mean Nusselt number and mean Darcy friction factor values for hexagonal-shaped cross-sectional channel with 60° side angle

Mesh number	45×10^3	100×10^3	250×10^3	510.3×10^3	998.4×10^3
Nu	110.59	109.49	106.49	106.02	106.27
f	0.0211	0.0202	0.0206	0.0205	0.0206

As can be seen in Table 1, mean Nusselt number and mean Darcy friction factor values change 0.02% and 0.0%, respectively, when the number of cell changes from 250×10^3 to 998.4×10^3. Since the change is less than 1%, the optimum mesh number for the hexagonal duct with 60° side angle is chosen as 250×10^3. Similarly, mesh optimization studies are conducted when side angle of the hexagonal duct is changed.

3. RESULTS AND DISCUSSION

3.1. Validation

To validate the solution of numerical study, turbulent flow in hexagonal duct with side angle of 90°, corresponding to rectangular channel with aspect ratio 2, is conducted. Local Darcy friction factor is given along the entrance and test sections of hexagonal cross-sectional channel in Fig. 3a. Fig. 3a shows that local Darcy friction coefficient initiates with a high value at the inlet of the entrance section channel, reduces along the hexagonal-shaped cross-sectional channel. It approaches to fully developed value, that is, constant value. Results indicate that the length of the entrance section channel is enough to obtain hydrodynamically fully developed flow conditions at the exit section. Results point out that local Darcy friction factor reduces with enhancing Reynolds number. Similarly, peripherally averaged local Nusselt number for test section is shown in Fig. 3b as a function of dimensionless duct length x/D_h for various Reynolds numbers. Results show that Nusselt number starts with a high value, decreases along the test section channel. Then it remains constant, that is, fully developed value. As expected, results indicate that Nusselt number enhances with rising Reynolds number.

At the fully developed conditions, Darcy friction coefficient and Nusselt number for hexagonal-shaped cross-sectional duct with $\theta=90^o$ are depicted as a function of Reynolds number and shown in Fig. 4. Fully developed values of Nusselt number and Darcy friction factor for $\theta=90^o$ are correlated in terms of Reynolds number and given as:

$$Nu_{fd} = 0.0336\,Re^{0.7421} \tag{18}$$

$$f_{fd} = 0.4676\,Re^{-0.2918} \tag{19}$$

Fully developed Fanning friction factor in a rectangular-shaped cross-sectional channel with aspect ratio 0.5 or 2.0 is given as [38-39]:

$$1/C_f{}^{0.5} = 4\log\left(1.029\,Re\,C_f{}^{0.5}\right) - 0.4 \tag{20}$$

Here C_f is the Fanning friction factor and $f=4C_f$. Darcy friction factor values obtained from Eq. (20) are also shown in Fig. 4a. The difference between the Eq. (19) and Eq. (20) is 3.6% and 4.3% for $Re=10\times10^3$ and $Re=50\times10^3$, respectively. Fully developed Nusselt number value for turbulent fluid flow in an isothermally heated rectangular cross-sectional channel is given by Rokni and Gatski [19] as $Nu_{fd}=30.4$ for Re=9397. As seen in Fig. 4a, fully developed Darcy friction factor reduces with enhancing Reynolds number. However, Nusselt number enhances with enhancing Reynolds number as seen in Fig. 4b. Fully developed Nusselt number of present study (i.e. Eq. (18)) for Re=9397 is 29.83. Results indicate that fully developed Nusselt number value of present study is about 1.9% less than that of the Rokni and Gatski [19]. That is, present numerical study is well agree with the literature results. In other words, numerical results obtained using standard k-ε turbulence model are in good agreement with the literature results.

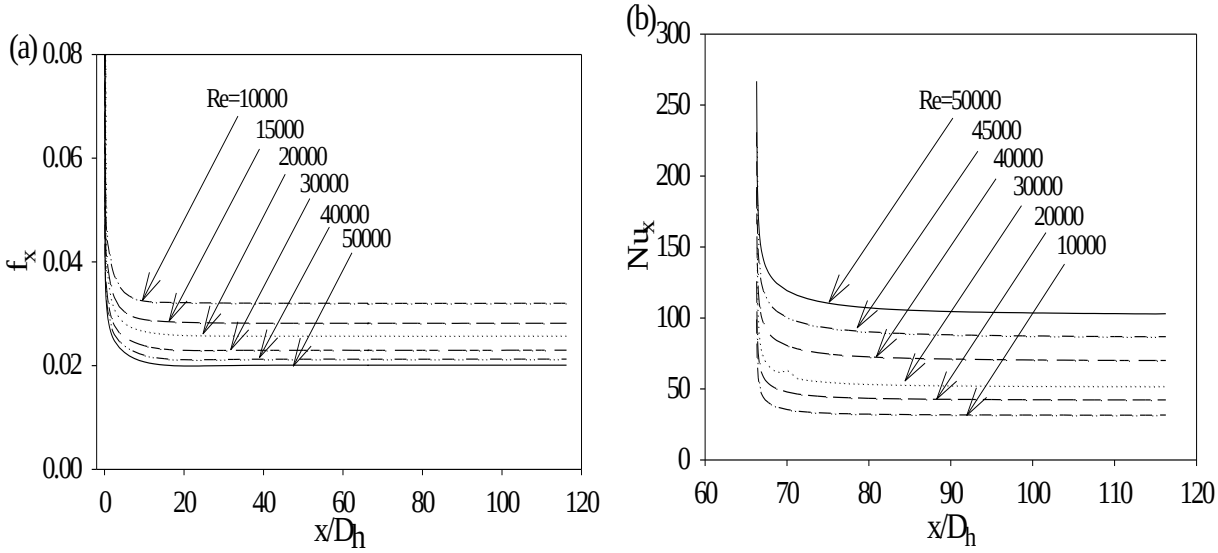

Figure 3. Local Darcy friction factor (a) and local Nusselt number at different Reynolds numbers along channel for $\theta=90^o$

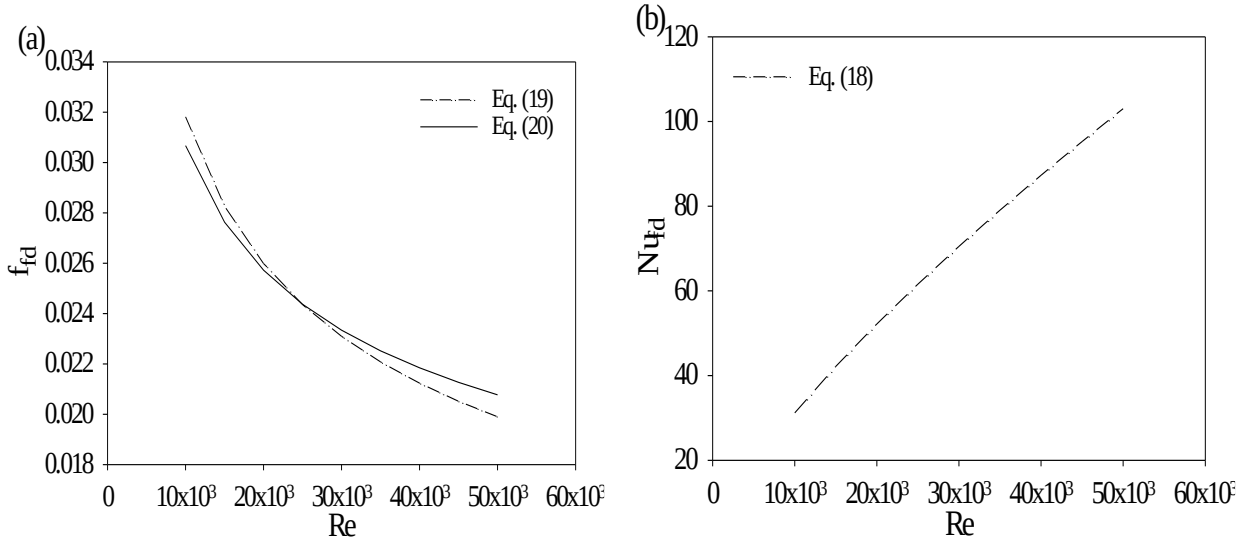

Figure 4. Darcy friction factor (a) and Nusselt number (b) values in terms of Reynolds number for θ=90°

3.2. Results

After validation of numerical solution method, numerical study is carried out for the hexagonal cross-sectional ducts with θ=30°, 45°, 60° and 75°. Fig. 5a shows the pressure drop along the hexagonal cross-sectional channel in terms of Reynolds number at different side angle θ values. Results indicate that the pressure drop along the duct rises logarithmically with enhancing flow velocity (therefore Reynolds number). Data provided in Fig. 5 reveal that regular hexagonal duct with the lateral angle of θ=60° has the lowest pressure drop along the duct while maximum pressure drop is obtained for the hexagonal cross-sectional duct with θ=30°. These results suggest that with minimum pressure losses, both pump operation head and shaft power will also be minimum for regular hexagonal duct with the lateral angle of θ=60°. Similarly, fully developed Darcy friction factor in a turbulent flow of hexagonal cross-sectional channel is depicted in terms of Reynolds number at five different side angle θ values in Fig. 5b. As expected, it is examined that peripherally averaged local Darcy friction coefficient reduces with rising Reynolds number.

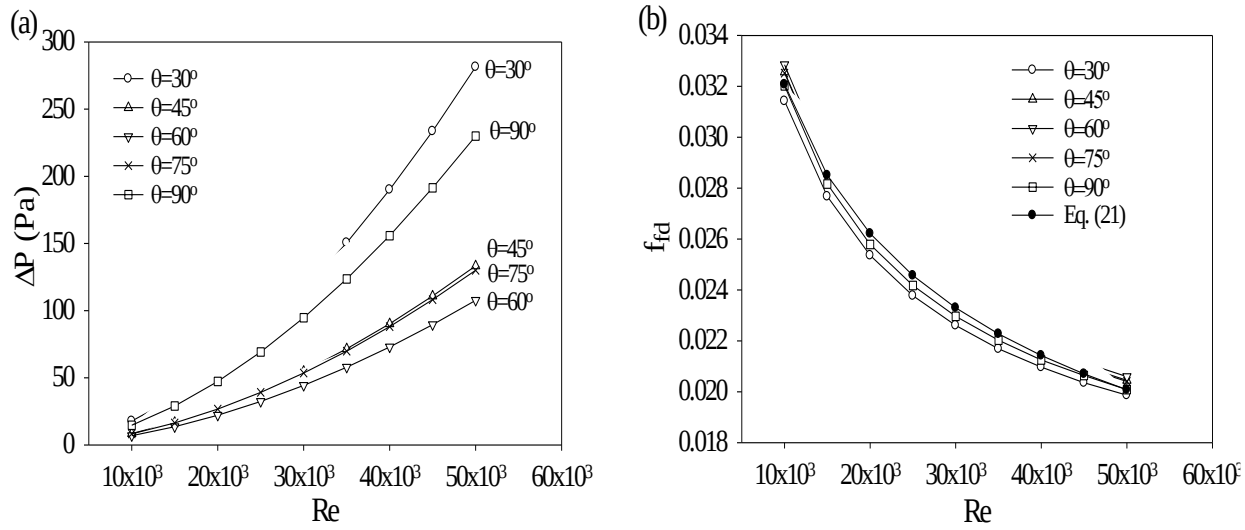

Figure 5. Pressure drop and (b) Darcy friction factor at different θ values

Fully developed Darcy friction coefficients for hexagonal cross-sectional duct with different side angles are correlated in terms of Reynolds number in the form of $f_{fd}=aRe^b$. The values of a and b correlation constants are given in Table 2. A general expression is given for Darcy friction coefficient between $30^o \le \theta \le 90^o$ and $10\times10^3 \le Re \le 50\times10^3$ as:

$$f_{fd} = 0.4684\,Re^{-0.2911} \quad (21)$$

Equation (21) represents the numerical values between -3.4% and + 2.5%. The values obtained from Eq. (21) is also plotted in Fig. 5b.

Table 2. The values of a and b constants for Darcy friction coefficient $f_{fd}=aRe^b$

θ	30°	45°	60°	75°	90°
a	0.4432	0.4736	0.4824	0.4756	0.4676
b	-0.2881	-0.2914	-0.2924	-0.2919	-0.2918

Convection heat transfer coefficient is shown in Fig. 6a in terms of Reynolds number at different side angles θ. As expected, convection heat transfer coefficient rises with enhancing Reynolds number. Nusselt number values for fully developed fluid flow are given in Fig. 6b in terms of Reynolds number at five different side angles θ. As can be seen from Fig. 6b, maximum Nusselt number is obtained for hexagonal cross-sectional channel with side angle $\theta=60^o$, i.e. regular hexagonal duct.

Fully developed Nusselt number values are correlated in terms of Reynolds number in the form of $Nu=cRe^d$, and the values of c and d correlation constants are given in Table 3.

Table 3. The values of c and d correlation constants of $Nu=cRe^d$

θ	30°	45°	60°	75°	90°
c	0.0303	0.0350	0.0365	0.0354	0.0336
d	0.7490	0.7400	0.7374	0.7393	0.7421

A general correlation is given for Nusselt number between $30^o \le \theta \le 90^o$ and $10\times10^3 \le Re \le 50\times10^3$ as:

$$Nu_{fd} = 0.0341\,Re^{0.7414} \quad (22)$$

Equation (22) represents the numerical values studied between –4.7% and +4.1%. The values obtained from Eq. (22) are also shown in Fig. 6b.

Fully developed Nusselt number and Darcy friction factor correlations for a regular hexagonal duct, i.e. $\theta=60^o$, were given by Turgut and Sari [22] for the Reynolds number range $11\times10^3 \le Re \le 52\times10^3$ using standard k-ε turbulence model, respectively, as:

$$Nu_{fd} = 0.034\,Re^{0.747} \quad (23)$$

$$f_{fd} = 0.421\,Re^{-0.277} \quad (24)$$

To compare the present results with the literature results, fully developed Nusselt number and Darcy friction factor values of present study and the results of Turgut and Sari [22] are shown in Fig. 7a and 7b, respectively, for a regular hexagonal duct. Results show that the maximum difference between present results and the results of Turgut and Sari [22] for Nusselt number and Darcy friction factor are 2.9% and, 1.9%, respectively. That is, present results are in good agreement with the results of Turgut and Sari [22].

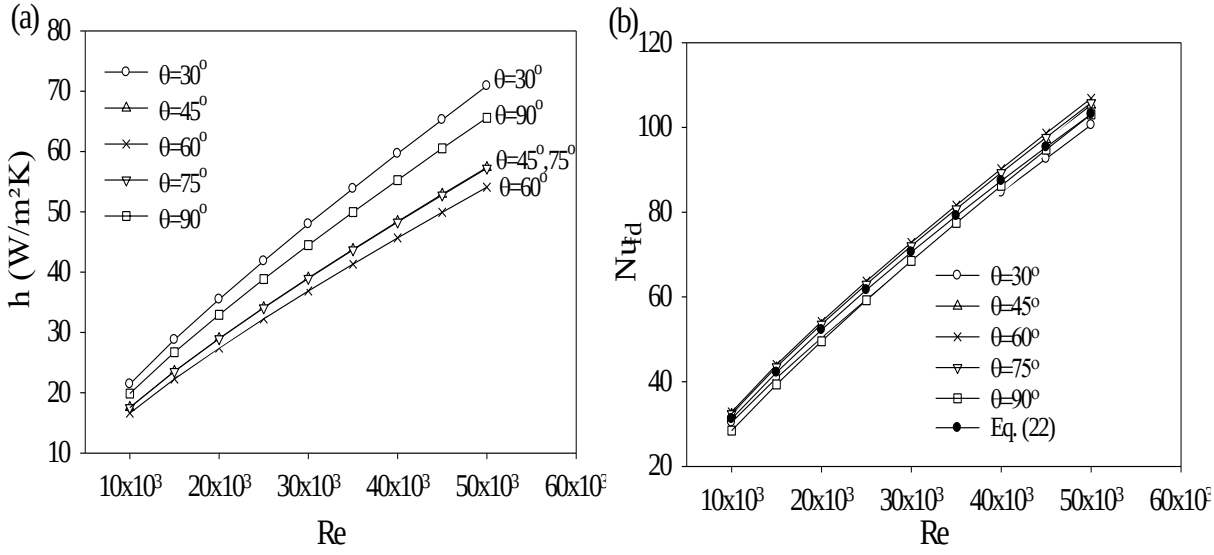

Figure 6. Fully developed heat transfer coefficient (a) and Nusselt number (b) at different side angles

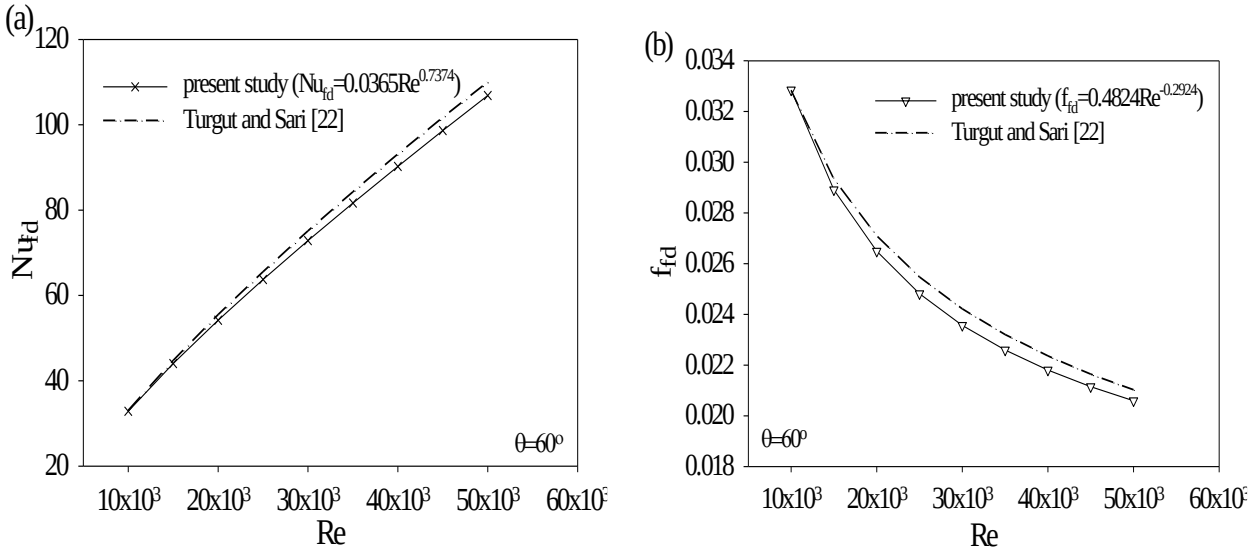

Figure 7. Comparison of present study results with literature (a) Nusselt number and (b) Darcy friction factor

To compare the present results with the literature results obtained from correlations derived for circular cross-sectional channels employing hydraulic diameter, the correlations at turbulent fully developed conditions for Nusselt number and Darcy friction factor expressions at fully developed flow are given in Table 4.

In order to see whether the correlations given for circular ducts in turbulent flow can be used for hexagonal cross-sectional ducts or not, fully developed Darcy friction factors obtained from Petukhov (Eq. (25)), Blasius (Eq. (26)) and Karman-Nikuradse (Eq. (27)) are plotted in Fig. 8a in terms of Reynolds number using hydraulic diameter of hexagonal cross-sectional channel. The results obtained from general equation Eq. (21) is also plotted in Fig. 8a. Results show that correlations obtained for turbulent flow in circular ducts can be used within 5% to obtain Darcy friction factor for a hexagonal cross-sectional duct using hydraulic diameter.

Likewise, fully developed Nusselt number values obtained from Colburn equation (Eq. (28)), Gnielinski equation (Eq. (29)) and Petukhov equation (Eq. (30)) are indicated in Fig. 8b in terms of Reynolds number using hydraulic diameter. Nusselt number values evaluated from general equation obtained for hexagonal cross-sectional channel, i.e. Eq. (22), are also sketched in Fig. 8b. As will be seen in Fig. 8b, correlations for circular ducts give the Nusselt number values within 14%. In addition, it is seen that Gnielinski correlation, i.e. Eq.(29), gives the Nusselt number within 5%.

Table 4. Expressions for Nusselt number and Darcy friction factor in a circular duct at fully developed turbulent fluid flow

$f_{fd} = (0.790 \ln Re - 1.64)^{-2}$	Petukhov	(25)
$f_{fd} = 0.316\, Re^{-0.25}$	Blasius	(26)
$1/C_f^{0.5} = 4\log\left(Re\, C_f^{0.5}\right) - 0.4$	Karman-Nikuradse	(27)
$Nu_{fd} = 0.023\, Re^{0.8}\, Pr^{1/3}$	Colburn	(28)
$Nu_{fd} = \dfrac{(f/8)(Re-1000)Pr}{1+12.7(f/8)^{0.5}\left(Pr^{2/3}-1\right)}$	Gnielinski	(29)
$Nu_{fd} = \dfrac{(f/8)\, Re\, Pr}{1.07+12.7(f/8)^{0.5}\left(Pr^{2/3}-1\right)}$	Petukhov	(30)

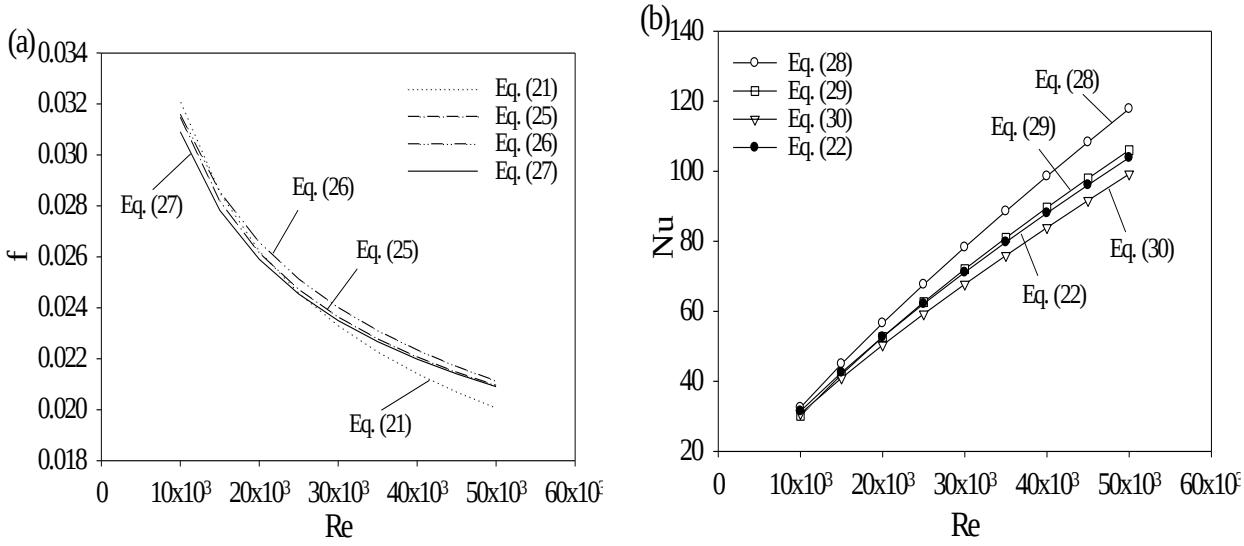

Figure 8. Comparison of Darcy friction factor (a) and Nusselt number (b)

General expressions in terms of Re and θ for fully developed Darcy friction factor and Nusselt number are obtained, respectively, as

$$f_{fd} = 0.4510\,\mathrm{Re}^{-0.2911}\left(\frac{180}{\pi\theta}\right)^{0.01028} \quad (31)$$

$$\mathrm{Nu}_{fd} = 0.03395\,\mathrm{Re}^{0.7414}\left(\frac{\pi\theta}{180}\right)^{0.01108} \quad (32)$$

Eq. (31) represents the numerical values studied between –6.0% and +0.2%, and Eq. (32) represents between –10.8% and +4.5%. In Eqs. (31) and (32), the angle θ is in degrees. Eqs. (31) and (32) are valid for $30^o \le \theta \le 90^o$ and $10\times10^3 \le \mathrm{Re} \le 50\times10^3$.

To compare the general correlation results for Darcy friction factor, i.e. Eqs. (21) and (31), and Nusselt number, i.e. Eqs. (22) and (32), with the actual hexagonal duct results obtained from Tables 2 and 3, Darcy friction factor and Nusselt number results are plotted in Fig. 9a and 9b, respectively, for $\theta=60^o$. It is seen that the results of general correlation of Darcy friction factor in the form of aRe^b, Eq. (21), deviates maximum -4.7% from actual hexagonal duct results. This deviation is -6.2% when the general correlation involves θ (please see Eq. (31)).

Similarly, it is concluded that the results of general correlation of Nusselt number in the form of cRe^d, Eq. (22), deviates maximum -3.5% from actual hexagonal duct results. This deviation is -3.1% when the general correlation involves θ (please see Eq. (32)).

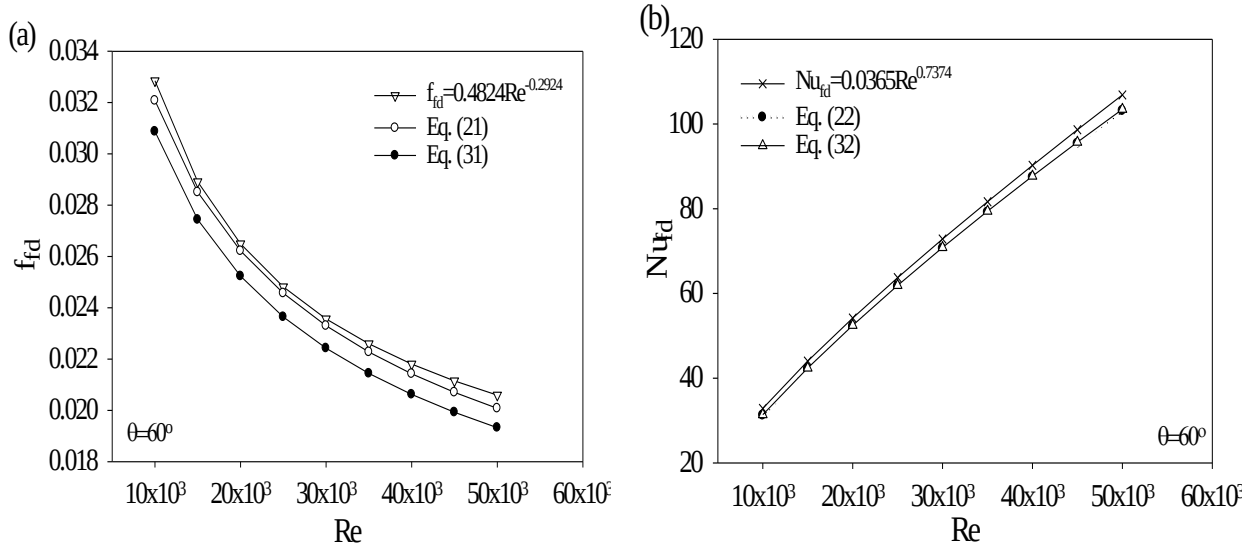

Figure 9. Comparison of general correlations with actual hexagonal duct for Darcy friction factor (a) and Nusselt number (b)

4. CONCLUSION

In this present study, the characteristics of turbulent heat transfer and fluid flow in hexagonal-shaped cross-sectional duct are numerically studied at constant wall temperature thermal boundary condition to see whether the fully developed turbulent flow correlations derived for circular ducts can be used for hexagonal cross-sectional ducts using hydraulic diameter. Reynolds number and side angle of the duct are the investigated parameters. Reynolds number changes between 10^4 and $5x10^4$. Side angle of the hexagonal duct is varied from 30^o and 90^o with an incremental of 15^o. Numerical study is implemented employing ANSYS Fluent 17.0 software program. The standard k-ε turbulence model is selected for numerical investigation. Based on the results of this numerical investigation for $10\times10^3 \leq Re \leq 50\times10^3$ and $30^o \leq \theta \leq 90^o$, general correlations in terms of Reynolds number and side angle θ are obtained for Nusselt number within –10.8% and +4.5% and Darcy friction factor within –6.0% and +0.2%. In order to see whether the correlations obtained for circular cross-sectional ducts can be used or not for hexagonal-shaped cross-sectional ducts using hydraulic diameter, comparison of the conclusions of present study are performed with the results of literature for circular cross-sectional channels. Results show that using the correlations of circular ducts for hexagonal ducts using hydraulic diameter may be 5% and 14% higher than that of actual hexagonal cross-sectional channels for Nusselt number and Darcy friction factor, respectively. It is found that Nusselt number enhances with rising Reynolds number. However, friction factor reduces with enhancing Reynolds number. Minimum pressure drop and maximum Nusselt number in hexagonal-shaped cross-sectional duct are obtained for regular hexagonal duct, $\theta=60^o$.

NOMENCLATURE

a-d	Correlation coefficients, -
A_s	Heat transfer surface area, m^2
C_f	Fanning friction factor, -
C_p	Specific heat, $J\cdot kg^{-1}\cdot K^{-1}$
D_h	Hydraulic diameter, m
f	Darcy friction coefficient, -
h	Heat transfer coefficient, $W\cdot m^{-2}\cdot K^{-1}$
k	Thermal conductivity of air, $W\cdot m^{-1}\cdot K^{-1}$
k	Turbulence kinetic energy, $m^2\cdot s^{-2}$
L	Duct length, m
$\dot{m}$	Mass flow rate of air, $kg\cdot s^{-1}$
Nu	Nusselt number, -
P	Pressure, Pa
ΔP	Pressure drop, Pa
Pr	Prandtl number, -
Re	Reynolds number, -
$\dot{q}''$	Heat flux, $W\cdot m^{-2}$
T	Temperature, K
u_i	i-direction velocity component, $m\cdot s^{-1}$
u_j	j-direction velocity component, $m\cdot s^{-1}$
U	Average velocity, $m\cdot s^{-1}$
x_i	Coordinate in the i-direction, m
x_j	Coordinate in the j-direction, m
y^+	Dimensionless distance to the wall, -
δ_{ij}	Kronecter delta, -
ε	Turbulence dissipation rate, $m^2\cdot s^{-3}$
μ	Dynamic viscosity of air, $kg\cdot m^{-1}\cdot s^{-1}$
θ	Side angle, ^{o}
ρ	Density of air, $kg\cdot m^{-3}$
τ	Shear stress, $N\cdot m^{-2}$

Subscripts

b	bulk
fd	fully developed
i	inlet
o	outlet
x	local
w	wall

DECLARATION OF ETHICAL STANDARDS

The authors of this article declare that the materials and methods used in this study do not require ethical committee permission and/or legal-special permission.

AUTHORS' CONTRIBUTIONS

Umut Baris YILMAZ: Performed the numerical analysis, analyzed the results and wrote the manuscript.

Oguz TURGUT: Analyzed the results and wrote the manuscript.

CONFLICT OF INTEREST

There is no conflict of interest in this study.

REFERENCES

[1] Kakac S, Shah R. K. and Aung W., Handbook of single-phase convective heat transfer. Wiley, USA, (1987).

[2] He S. and Gotts J. A., "Calculation of friction coefficients for noncircular channels", ***Journal of Fluids Engineering - Transactions of the ASME***, 126: 1033-1038, (2004).

[3] Sadasivam R., Manglik R. J. and Jog M. A., "Fully developed forced convection through trapezoidal and hexagonal ducts", ***International Journal of Heat and Mass Transfer*** , 42: 4321-4331, (1999).

[4] Shah R. K. and London A. L., "Laminar flow forced convection in ducts", in: Irvine T. F. and Harnett J. P., ***Academic Press***, New York, (1978).

[5] Shah R. K. and Bhatti M. S., "Laminar convective heat transfer in ducts", in: Kakaç S., Shah R. K. and Aung W., ***Wiley***, New York, (1978).

[6] Asako Y., Nakamura H. and Faghri M., "Developing laminar flow and heat transfer in the entrance region of regular polygonal ducts", ***International Journal of Heat and Mass Transfer***, 31: 2590-2593, (1988).

[7] Damean N. and Regtien P. P. L., "Velocity field of the fully developed laminar flow in a hexagonal duct", ***Sensors and Actuators A: Physical***, 92: 144-151, (2001).

[8] Oztop H. P., Sahin A. Z. and Dagtekin I., "Entropy generation through hexagonal cross-sectional duct for constant wall temperature in laminar flow", ***International Journal of Energy Research***, 28: 725-737, (2004).

[9] Nonino C., Del Giudice S. and Savino S., "Temperature dependent viscosity effects on laminar forced convection in the entrance region of straight ducts", ***International Journal of Heat and Mass Transfer***, 49: 4469-4481, (2006).

[10] Jarungthammachote S., "Entropy generation analysis for fully developed laminar convection in hexagonal duct subjected to constant heat flux", ***Energy***, 35: 5374-5379, (2010).

[11] Saksena D.P., "Entropy generation analysis for fully developed laminar convection in hexagonal duct subjected to constant heat flux and minimization of entropy generation by adjusting the shape of the cross section", ***International Journal of Engineering Science Invention (IJESI)***, 2: 17-29, (2013).

[12] Haghgooyan M. S. and Aghanajafi C., "Entropy generation analysis for various cross-sectional ducts in fully developed laminar convection with constant wall heat flux", ***Korean Chemical Engineering Research***, 52: 294-301, (2014).

[13] Turgut O., "Numerical investigation of laminar flow and heat transfer in hexagonal ducts under isothermal and constant heat flux boundary conditions", ***Iranian Journal of Science and Technology: Transactions of Mechanical Engineering***, 38: (M1), 45-56, (2014).

[14] Yadav R. J., Kore S., Raibhole V. N. and Joshi P.S., "Development of correlations for friction factor and heat transfer coefficient for square and hex duct with twisted tape insert in laminar flow", ***Precedia Engineering***, 127: 250-257, (2015).

[15] Arani A. A. A., Arefmanesh A. and Niroumand A., "Investigation of fully developed flow and heat transfer through n-sided polygonal ducts with round corners using the Galerkin weighted residual method", ***Internationa Journal of Nonlinear Analysis And Applications***, 9: 175-193, (2018).

[16] Sajjad E. and Mohammad H. D. B., Mohammad M., Hamid M. and Maisam S., "Comparison of heat transfer and fluid flow in the micro-channel with rectangular and hexagonal cross section", ***Archives for Technical Sciences***, 21: 1-10, (2019).

[17] Emami S., Bonab M. H. D., Mohammadiun M., Mohammadiun H. and Sadi M., "Evaluation of Nusselt number and pressure drop in hexagonal and rectangular micro-channels in the presence of nano-fluids", ***Proceedings of the Institution of Mechanical Engineers, Part E: Journal of Process Mechanical Engineering***, doi: doi.org/10.1177/0954408920935725

[18] Iwaniszyn M., Jodłowski P. J., Sindera K., Gancarczyk A., Korpyś M., Jędrzejczyk R. J. and Kołodziej A., "Entrance effects on forced convective heat transfer in laminar flow through short hexagonal channels: experimental and CFD study", 405: doi: doi.org/10.1016/j.cej.2020.126635

[19] Rokni M. and Gatski T. B., "Predicting turbulent flow and heat transfer", ***In Proceedings of the 3rd International Symposium on Turbulence, Heat and Mass Transfer***, Nagoya, Japan, 357-364, (2000).

[20] Sari M., "Experimental investigation of forced convection heat transfer in hexagonal duct with turbulent flow conditions", ***MSc. Thesis***, Gazi University, Graduate School of Natural and Applied Sciences, (2010).

[21] Can O.F., Celik N. and Dagtekin I., "Investigation of flow and heat transfer in hexagonal channels with different geometries", ***Conference paper: 2nd Anatolian Energy Symposium***, (8 pages), Turkey, (2013).

[22] Turgut O., Sari M., "Experimental and numerical study of turbulent flow and heat transfer inside hexagonal duct", ***Heat Mass Transfer***, 49: 543-554, (2013).

[23] Wang P., Yang M., Wang Z. and Zhang Y., "A new heat transfer correlation for turbulent flow of air with variable properties in noncircular ducts", ***Journal of Heat Transfer - Transactions of the ASME***, 136: 101701 (8 pages), (2014).

[24] Opute E. K., "Empirical investigation of the laminar thermal entrance region and turbulent flow heat transfer for non-Newtonian silica nanofluid in hexagonal tubes", ***MSc. Thesis***, University of North Dakota, Graduate Faculty, (2015).

[25] Falih A. H., "Thermal and hydraulic response of turbulent flow inside hexagonal duct fitted with various inserts", ***Wasit Journal of Engineering Science***, 4: 147-162, (2016).

[26] Marin O., Vinuesa R., Obabko A. V. and Schlatter A., "Characterization of the secondary flow in hexagonal ducts", ***Physics of Fluids***, 28: 125101 (28 pages), (2016).

[27] Gunes S., Ozceyhan V., Dagdevir T. and Keklikcioglu O., "Numerical investigation of heat transfer enhancement in a tube with hexagonal cross sectioned coiled wire", ***International Journal of Mechanical And Production Engineering (IJMPE)***, 5: 96-100, (2017).

[28] Mahato S. K., Rana S. C., Barman R. N. and Goswami S., "Numerical analysis of heat transfer and fluid flow through twisted hexagonal and square duct and their comparisons", ***Chemical Engineering Transactions***, 71: 1351-1356, (2018).

[29] Yadav R. J., Kore S. S. and Joshi P. S., "Correlations for heat transfer coefficient and friction factor for turbulent flow of air through square and hexagonal ducts with twisted tape insert", ***Heat and Mass Transfer***, 54: 1467-1475, (2018).

[30] Aolin G. J. X. and Cai Z. H., "An investigation of developing flow and heat transfer in a triangular duct" ***Journal of Shanghai Institute of Mechanical Engineering***, 11(4): 1-12, (1989).

[31] Rokni M., Sunden B., "Numerical investigation of turbulent forced convection in duts with rectangular and trapezoidal cross-section area by using different turbulence models", Numerical Heat Transfer - Part A, 30: 321-346, (1996).

[32] Bardina, J.E., Huang, P.G., Coakley, T.J., "Turbulence modeling validation, testing, and development***", NASA Technical Memorandum***, 110446, (1997).

[33] Wang L. B., Wang Q. W., He Y. L. and Tao W. Q., "Experimental and numerical study of developing

turbulent row and heat transfer in convergent/divergent square ducts", ***Heat and Mass Transfer***, 38: 399-408, (2002).

[34] Albets-Chico X., Perez-Segarra C. D., Oliva A. and Bredberg J., "Analysis of wall-function approaches using two-equation turbulence models", ***International Journal of Heat and Mass Transfer***, 51: 4940-4957, (2008).

[35] Yilmaz U. B., "Numerical investigation of hydrodynamically fully developed, thermally developing flow in hexagonal duct", ***MSc. Thesis***, Gazi University, Graduate School of Natural and Applied Sciences, (2012).

[36] ANSYS Fluent 17.0, Theory Guide, ***ANSYS Inc***., (2016).

[37] Incropera F. P., DeWitt D. P., Theodore L. B. and Adrienne S. L., "Principles of heat and mass transfer", ***John Wiley and Sons Inc***., Singapore, (2013).

[38] Ward-Smith A. J., "Internal Fluid Flow: The Fluid Dynamics of Flow in Pipes and Ducts", ***Clarendon Press***, Oxford, (1980).

[39] Harnett J. P. and Kostic M., "Heat transfer to newtonian and non-newtonian fluids in rectangular ducts", ***Advances in Heat Transfer***, 19: 247-356, (1989)